EFFECT OF TEMPERATURE, PRESSURE AND VOLUME OF REACTING PHASE ON PHOTOCATALYTIC CO_2 REDUCTION ON SUSPENDED NANOCRYSTALLINE TiO_2

Kamila KOČÍ[a1,*], Lucie OBALOVÁ[a2], Daniela PLACHÁ[b1] and Zdenek LACNÝ[b2]

[a] *Department of Physical Chemistry and the Theory of Technological Processes, Faculty of Metallurgy and Material Engineering, Technical University Ostrava, 17. listopadu 15, 708 33 Ostrava, Czech Republic; e-mail:* [1] *kamila.koci@vsb.cz,* [2] *lucie.obalova@vsb.cz*

[b] *Nanotechnology Centre, Technical University Ostrava, 17. listopadu 15, 708 33 Ostrava, Czech Republic; e-mail:* [1] *daniela.placha@vsb.cz,* [2] *zdenek.lacny@vsb.cz*

Received May 3, 2008
Accepted August 11, 2008
Published online October 3, 2008

The effect of temperature, pressure and volume of reactant solution on the photocatalytic reduction of CO_2 at suspended TiO_2 was studied in an annular batch photoreactor. Reaction products in the liquid phase (methanol, formaldehyde) and in the gas phase (methane, ethane, carbon monoxide, molecular oxygen and hydrogen) were analysed by gas chromatography. The photocatalytic reduction of CO_2 was not sensitive significantly to small temperature variations within 10 K. The CO_2 pressure at carbonation of the solution influenced the selectivity of the CO_2 conversion to methane and methanol, while the dihydrogen yield was higher by two orders of magnitude and independent of the pressure. The dependence of the product yields on the volume of the liquid phase confirmed the fact that the requirement for perfect mixing was difficult to fulfil for the annular configuration of the reactor.

Keywords: Carbon dioxide; Photocatalysis; Reduction; Titanium dioxide; Temperature effect; Pressure effect.

Photocatalysis can be defined as an acceleration of a photoreaction in the presence of a catalyst. Unlike metals, that feature a continuum of electronic states, semiconductors exhibit a void energy region, or a band gap that extends from the top of the filled valence band (VB) to the bottom of the vacant conduction band (CB). The photocatalysis over semiconductors is initiated by absorption of a photon having an energy equal to or greater than the band gap of the semiconductor, producing electron–hole (e^-/h^+) pairs. Consequently, following the irradiation, the catalyst particle can act either as an electron donor or an acceptor for molecules in the surrounding

doi:10.1135/cccc20081192

medium. However, the photoinduced charge separation in the bare catalyst particles has a very short lifetime (typically a few nanoseconds) because of a rapid charge recombination. It is therefore important to prevent the hole–electron recombination before a certain desired chemical reaction occurs at the catalyst surface.

In addition to properties of a particular semiconductor and its surface modification, other reaction variables play an important role in determining the reaction rate and the extent of reactant transformation. They include the semiconductor catalyst concentration, apparent reactive surface area, porosity of aggregates, concentration of electron donors and acceptors, incident light intensity, pH value, presence of competitive sorbates, temperature and pressure. The influence of some of these parameters has already been described in[1,2].

Furthermore, the overall rate of the reactant conversion can be influenced by macrokinetic phenomena (mass and heat transfer and properties of the experimental reactor). The careful choice of experimental conditions to avoid the macrokinetic phenomena is important and necessary for the comparison of experimental data between laboratories and their application for a large equipment.

From the point of view of the phases involved, photocatalysis in a gas phase (e.g., photocatalytic NO_x reduction[3–5], destruction of gaseous organic pollutants – photodeodourisation and self-cleaning photofilms[6,7]), photocatalysis in a liquid phase (e.g., photocatalytic oxidation of organic compounds[8–10]) and photocatalysis with participation of both gas and liquid phases (e.g., photocatalytic reduction of CO_2 [11,12], photoreduction of N_2 [13]) can be distinguished.

Hereof, a photocatalytic reaction with the participation of gas and liquid phases is the most complex one with regard of possible macroscopic phenomena. The reaction rate and selectivity can be influenced in this case by a mass transport from the bulk of the gas to the gas–liquid phase boundary, by dissolved gas diffusion in the liquid to the external catalyst surface, by an internal mass transport in the catalyst pores or agglomerates, by phase equilibria and transfer of light radiation.

The problem of mass transfer limitations in slurry photocatalytic reactors employing titanium dioxide was discussed in a comprehensive work of Ballari and co-workers[14,15]. Even though major differences exist between reactions proceeding in a liquid phase only and gas–liquid phase reactions where the gas must first dissolve prior to its destruction, some conclusions of these investigations are also applicable to the gas–liquid reaction in stirred batch reactors with a suspended TiO_2 catalyst.

Ballari et al.[14] concluded that concentration gradients in the bulk of a stirred liquid with suspended TiO_2 could be avoided for a catalyst loading under 1 g dm^{-3}, good mixing conditions, low reaction rate and irradiation rate below 10^{-7} Einstein cm^{-2} s^{-1}. Sasirekha et al.[16] and Tseng et al.[17] published as well that the concentration of the suspended TiO_2 catalyst should be kept below 1 g dm^{-3} to avoid light scattering caused by the high TiO_2 concentration, which hinders light from reaching every catalyst particle.

Interfacial external mass transfer limitations in the boundary layer surrounding the catalytic particle could be observed only for rather large particles, usually not encountered in suspended TiO_2. However, inside the catalytic particle or the porous agglomerate, restriction of the light penetration can be observed even for particle sizes (or agglomerates) below 1 μm [15] and the reaction rate then can not be considered under the kinetic control regime.

The photocatalytic reduction of CO_2 in a gas–liquid slurry batch reactor with TiO_2 catalyst was the subject of this study. This reaction is one of the most promising ways to reduce CO_2 emitted for example by fossil fuel combustion, to useful compounds (methanol, ethanol, formic acid, formaldehyde, methane, etc.) by UV radiation. Regardless numerous investigations in this area, photocatalytic CO_2 reduction is still far from practical applications[18]. Optimisation of reaction conditions (temperature, pressure, pH, light intensity) is another possibility besides the selection of proper catalyst and reductant to improve efficiency of the photocatalytic process.

In the case of photocatalysts, photon radiation is the primary source of energy for the electron–hole pair formation at ambient temperature, as the band-gap energy is too high for thermal excitation to overcome. However, it is clear that the photocatalytic reactions proceed more efficiently at high temperatures because the reaction rate can be increased by raising the collision frequency and diffusion rate. Anpo et al.[19] studied the effect of temperature on the photocatalytic CO_2 reduction and observed that the total yields of CH_4, CH_3OH and CO are higher under UV irradiation at 323 K than at 275 K. On the other hand, Fox et al.[2] concluded that photocatalytic reactions are not sensitive significantly to small temperature variations, with some exceptions. Kohno et al.[20] studied CO_2 photocatalytic reduction and demonstrated that the increase of the reduction temperature above 523 K resulted in a drastic decrease of the CO production while CH_4 production slightly increased, which means that variation of the reaction temperature may also influence the catalyst selectivity.

The concentration of CO_2 dissolved in water is low. Increasing the CO_2 pressure is one of the means of increasing the concentration of CO_2 dissolved in water and, thus, improving CO_2 reduction selectivity. Mizuno et al.[12] published that the photocatalytic reduction of CO_2 accelerated by the increased CO_2 pressure preferentially yields liquid products and an optimum CO_2 pressure exists for the formation of methanol. The yield of the liquid reduction products was roughly one order of magnitude higher than that of the gaseous products. Tseng et al.[17] quoted that the methanol yield clearly increased with the increase of the CO_2 pressure up to 125 kPa, but decreased above this pressure value. The effect of the CO_2 pressure on its photocatalytic reduction using a TiO_2 suspension in isopropanol was also investigated[21]. The results illustrate that the formation of methane increased with the CO_2 pressure elevated up to 2.8 MPa.

The elimination of CO_2 diffusion from the bulk of gas through the gas–liquid interface in a laboratory batch slurry reactor is reached by saturation of the liquid by CO_2 before the reaction starts[12,17]. Aqueous NaOH is often used as a reductant environment in this reaction. There are two reason for it: (i) increasing the amount of dissolved CO_2 because caustic NaOH solution dissolves more CO_2 than pure water and (ii) reducing the recombination of hole–electron pairs leading to the longer decay time of surface electrons, and facilitating the CO_2 reduction because the OH^- ions in the concentrated aqueous solution could act as strong hole-scavengers transforming to $^{\bullet}OH$ radicals. The optimum concentration of NaOH was reported as 0.2 mol l^{-1} (refs[17,21]).

Although there are some studies dealing with temperature and pressure effect on the photocatalytic CO_2 reduction, the results are inconsistent. The fact, that only a few authors analysed both the liquid and gaseous products, could be the reason. An additional question regards the influence of gas and liquid volume variation on the reaction yield and selectivity. The aim of this study is to assess the effect of temperature, pressure and the volume of reactant solution on photocatalysis exemplified by the photoreduction of CO_2 at suspended TiO_2.

EXPERIMENTAL

TiO_2 Preparation and Characterisation

TiO_2 particles were prepared by the sol-gel method controlled in inverse micellar environment of Triton X-114 (Aldrich) in cyclohexane.

The prepared TiO_2 powder was characterised by various techniques to specify the structural and textural properties: the crystalline phase and crystallite size by X-ray diffraction (XRD),

the specific surface area by nitrogen physical adsorption at 77 K, and the chemical composition and morphology by scanning electron microscopy (SEM).

The XRD measurement was performed using a Seifert-FMP laboratory diffractometer with a Cu anode in the conventional focusing Bragg–Brentano experimental arrangement in the measured range $2\theta = 10–105°$.

An adsorption apparatus ASAP2020 (Micromeritics, U.S.A.) was used for the determination of the specific surface area by the nitrogen physical adsorption at 77 K. Prior to the adsorption measurement, all samples were degassed at 110 °C until the pressure of 0.1 Pa was attained (ca. 12 h).

UV-VIS absorption spectra were recorded on a Varian Cary 100 spectrophotometer. The TiO_2–water suspension was used for the measurement.

Photocatalytic Reactivity Experiments

The photocatalytic reduction of carbon dioxide was carried out in a homemade apparatus (Fig. 1).

A stirred batch annular reactor with the suspended catalyst was illuminated by an 8 W Hg lamp (Ultra-Violet Products, U.S.A.) with a peak light intensity at 254 nm, situated in the centre of a quartz tube. The shell tube was made of stainless steel. The catalyst powder (1 g dm^{-3}) was suspended in 0.2 M NaOH for all batches. Supercritical-fluid grade CO_2 with certified maximum of hydrocarbons less than 1 ppm (SIAD Technical Gases, Czech Republic) was used as the reactant to avoid any hydrocarbon contamination. A magnetic stirrer at the bottom agitated the catalyst suspension to prevent any sedimentation of the catalyst. The temperature and pH of the solution and the pressure of the gas phase were continuously monitored (Digital Pressure Meter GMH 3110, Digital pH-Thermometer GMH 3530).

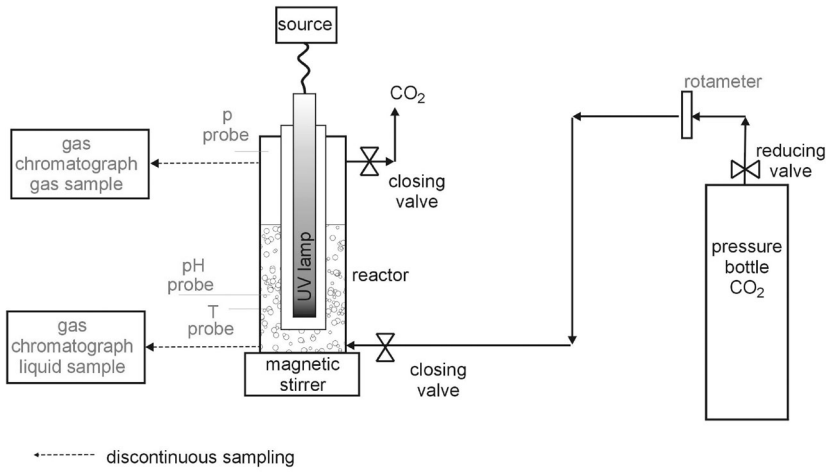

FIG. 1
Block scheme of the employed apparatus for photocatalytic CO_2 reduction

Prior to illumination, CO_2 was bubbled at constant flow and a pressure in the range of 100–130 kPa through the stirred suspension for at least 45 min to purge on air and to saturate the solution. The reactor was then tightly closed and the CO_2 pressure was maintained steady. After that, the photocatalytic reaction was started by triggered irradiation with the Hg lamp.

The samples of gas and liquid reaction mixture were taken after 24 h of irradiation. Small aliquots of the suspension were withdrawn by syringe, filtered through a Millipore filter membrane and analysed. Gas sampling was performed with a gas-tight syringe (10 ml) through a septum and samples were analysed immediately.

Blank reactions were conducted to ensure that hydrocarbon production was due to the photoreduction of CO_2 and to eliminate surrounding interference. One blank was UV-illuminated without the catalyst, and another one was kept in the dark with the catalyst and CO_2 under the same experimental conditions. No hydrocarbons were detected in the above blank tests.

Analyses

Gas phase samples were analysed using a gas chromatograph (GC-Agilent Technologies 6890 N) equipped with FID, TCD detectors and a Molsieve and HP Poraplot Q column for methane, hydrogen, ethane, carbon monoxide, carbon dioxide, oxygen and nitrogen analyses. A calibration with certificated calibration gases (1.5 mole % CH_4, 0.987 mole % H_2, 2.02 mole % CO, 99.999 mole % CO_2) was performed before each experimental run. Samples of liquid phase were analysed in a gas chromatograph (GC-Agilent Technologies 6890 N) equipped with an FID detector and an HP 5 column for methanol and ethanol analyses. Five-point calibration using standard samples was performed. Helium was used as the carrier gas in the case of both GC. In the present study, the modified method for colorimetric formaldehyde determination with chromotropic acid was investigated. Sample aliquots were reacted with chromotropic acid in the presence of sulfuric acid to form a purple monocationic chromogen. A Hatch DR 900 spectrophotometer was used for all absorbance measurements. The five-point calibration was prepared by plotting absorbance against formaldehyde concentration for each calibration level.

RESULTS AND DISCUSSION

Catalyst Characterization

The prepared TiO_2 catalyst was characterised by XRD. The surface area and porous structure were determined by adsorption/desorption of nitrogen at 77 K. The only crystalline phase was semi-anatase with crystallite size of 6 nm. Specific surface area evaluated by BET method was 86.5 $m^2\ g^{-1}$. The sample contained relatively large volume of micropores (16.9 $mmliq^3\ g^{-1}$); the average pore radius was 1.8 nm.

Figure 2 shows the electronic absorption spectra of the TiO_2 powder. The TiO_2 catalyst (6 nm) exhibits a large absorption band below 400 nm. The UV-VIS spectrum exhibits a rather narrow absorption band at 218 nm at-

tributed to Ti(IV) species in a tetrahedral coordination environment and a broad band between of 330–400 nm, which indicates the anatase phase of TiO_2 [16]. The absorption edge was determined as 405 nm.

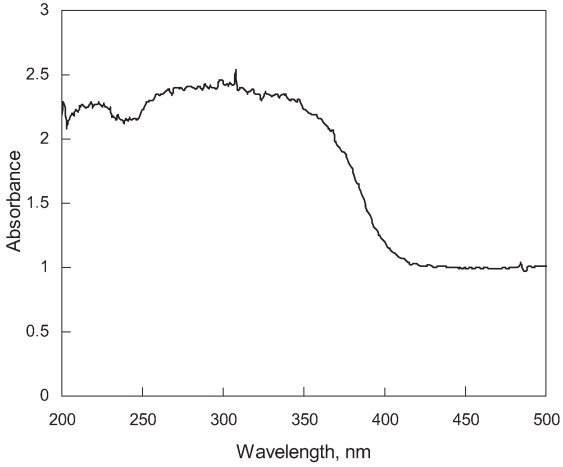

FIG. 2
UV-VIS absorbtion spectrum of the TiO_2 catalyst

Photocatalytic Reduction of CO_2

Various reaction schemes for the photocatalytic reduction of CO_2 by H_2O at the TiO_2 catalysts have been proposed in the literature[16,19,21–24]. The process could consist of a series of reforming reactions described by Eqs (*1*)–(*11*), driven by UV irradiation of the catalyst and reactants.

$$TiO_2 \xrightarrow{h\nu} e^- (TiO_2) + h^+ (TiO_2) \qquad (1)$$

$$[(Ti^{4+}–O^{2-}) \xrightarrow{h\nu} (Ti^{3+}–O^-)^*] \qquad (2)$$

$$e^- (TiO_2) + h^+ (TiO_2) \xrightarrow{h\nu} \text{heat} \qquad (3)$$

$$h^+ + H_2O_{ads} \xrightarrow{hv,\ (Ti^{3+}–O^-)^*} {}^{\bullet}OH + H^+ \quad (4)$$

$$3\ h^+ + {}^{\bullet}OH + H_2O_{ads} \xrightarrow{hv,\ (Ti^{3+}–O^-)^*} O_2 + 3\ H^+ \quad (5)$$

$$H^+ + e^- \xrightarrow{hv,\ (Ti^{3+}–O^-)^*} H^{\bullet} \quad (6)$$

$$CO_2 + e^- \xrightarrow{hv,\ (Ti^{3+}–O^-)^*} CO_2^{\bullet-} \quad (7)$$

$$CO_2^{\bullet-} + 8\ H^{\bullet} + h^+ \xrightarrow{(Ti^{3+}–O^-)^*} CH_4 + 2\ H_2O \quad (8)$$

$$CO_2^{\bullet-} + 2\ H^{\bullet} + h^+ \xrightarrow{(Ti^{3+}–O^-)^*} CO + H_2O \quad (9)$$

$$CO_2^{\bullet-} + 4\ H^{\bullet} + h^+ \xrightarrow{(Ti^{3+}–O^-)^*} HCHO + H_2O \quad (10)$$

$$CO_2^{\bullet-} + 6\ H^{\bullet} + h^+ \xrightarrow{(Ti^{3+}–O^-)^*} CH_3OH + H_2O \quad (11)$$

When illuminated by UV light of sufficient energy ($h\nu$), photon-generated electrons (e^-) and holes (h^+) are created on the surface of the TiO_2 catalysts, Eqs (*1*)–(*3*) (Fig. 3). Furthermore, the photoexcited electrons and holes in the lattice are separated and trapped by appropriate sites of TiO_2 to avoid recombination. The holes first react with water adsorbed on the catalyst, resulting in the production of hydroxyl radicals ($^{\bullet}OH$) and protons (H^+) according Eq. (*4*). Water is further oxidised by $^{\bullet}OH$, producing molecular oxygen and H^+ (Eq. (*5*)). The interaction of H^+ with the excited electron in $(Ti^{3+}–O^-)^*$ leads to the formation of atomic H (Eq. (*6*)). At the same time, radicals $CO_2^{\bullet-}$ are formed from CO_2 (Eq. (*7*)). These incipient radicals $CO_2^{\bullet-}$ and $H^{\bullet}$ then react with each other, finally producing CH_4, CO, HCHO, CH_3OH (Eqs (*8*)–(*11*)). Generated dioxygen (Eq. (*5*)) can be partially con-

sumed in the reoxidation of methane. Tan et al.[25] demonstrated that incipient O_2 could cause reverse photooxidation of the products to carbon dioxide. This process may affect the initial reduction routes and limit the corresponding yields.

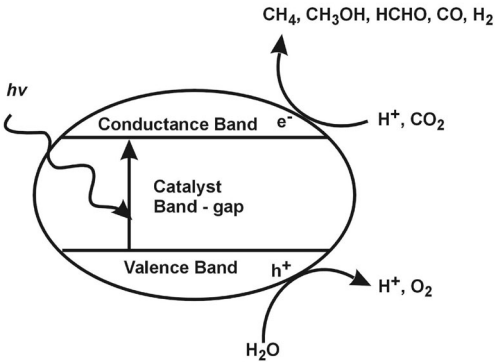

FIG. 3
Schematic model showing the photocatalysed reduction of CO_2 at TiO_2

Effect of Temperature

Two experiments were performed to check the temperature effect in the initial period of the photocatalytic CO_2 reduction. First, the NaOH solution with TiO_2 was tempered to the final temperature of 309 K, saturated by CO_2 and then irradiated with the UV lamp. In the second experiment, the CO_2 saturation took place at the laboratory temperature of 299 K. The temperature gradually increased along with the UV irradiation and the steady state temperature of 309 K was reached after 4 h. The product yields were the same in both experiments.

The temperature can have two effects in the (photo)catalytic gas–liquid–solid system: (i) influences the rate of chemical reactions, the kinetic rate constants usually increasing exponentially with temperature and (ii) determines the equilibrium amount of dissolved CO_2. Experimental results showed that the temperature increase of 10 K did not influence the rate of the photocatalytic CO_2 reduction considerably. The low reaction yields in the first 4 h of irradiation and their variation below detection limits could be the reason for this negative observation. Fox et al.[2] stated as well that majority of photocatalytic reactions is largely insensitive to small variations of temperature.

Effect of CO_2 Pressure

Figure 4 shows the dependence of product yields on CO_2 pressure at carbonation. Methanol was the only product in the liquid phase. Formaldehyde and ethanol were not detected. Methane, hydrogen and carbon monoxide were detected in the gas phase. No higher hydrocarbons were found in the gas phase. Hydrogen yields were roughly two orders of magnitude higher than those of the other products.

The amount of formed methanol was increasing with CO_2 pressure up to 130 kPa. Higher CO_2 pressure then caused a drop in the methanol yield. This trend of methanol formation in the liquid phase corresponds with results of Tseng et al.[17]. The methane yield in the gas phase showed an opposite trend: a decrease with increasing pressure up to 130 kPa and then an increase. This trend can not be compared with Tseng results as this group did not perform any analysis of the gas phase. The analysis of gaseous and liquid products of the photocatalytic CO_2 reduction was performed by Mizuno et al.[12]. Their results are quite different from our data: no methane was detected at atmospheric pressure and started to form at 1 MPa and higher CO_2 pressures. Figure 4 shows that the higher yields of methanol in the liquid phase lowered the methane yields in the gas phase and vice versa.

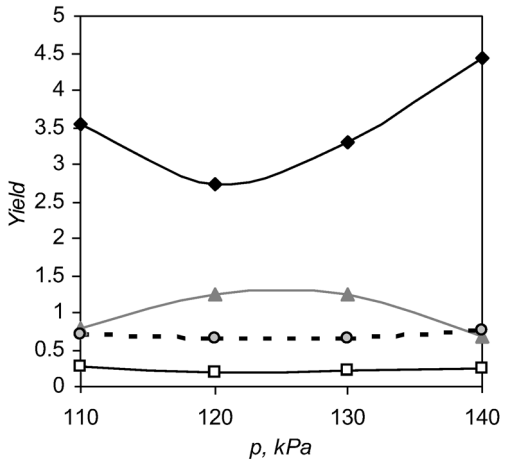

FIG. 4
Dependence of product yields (μmol g_{cat}^{-1}) on the CO_2 pressure (p) at carbonation: CH_4 (◆), CO (□), CH_3OH (▲), $H_2/100$ (●). Conditions: irradiation time 24 h, 8 W Hg lamp, 150 ml of 0.2 M NaOH, 0.15 g of catalyst

The yields of CO did not change with increasing CO_2 pressure and amounts of CO formed are close to detection limits. Also the amount of photogenerated H_2 is independent of the pressure at carbonation. The formation of molecular hydrogen is the result of recombination of hydrogen radicals. These radicals are produced by simultaneous photocatalytic water splitting (Eqs (*4*) and (*6*)). A part of them is consumed in the formation of CO_2 reduction products (CH_4 and CH_3OH, Eq. (*8*) and Eq. (*11*), respectively), but a major part transforms into H_2. The amount of CO_2 reduction products is two orders of magnitude lower then the yield of molecular hydrogen, which is almost invariable.

Effect of Liquid Phase Volume

Five experiments with different volumes of the liquid phase were performed. The dependence of product yields on this parameter is depicted in Fig. 5. It is clear that the ratio between the liquid and gas phase volumes influences the yields of gaseous and liquid products. The yields of all products increase with decreasing the liquid phase volume down to 100 ml. An insufficient mixing of the liquid phase at larger volumes, especially in a narrow annular space, is proposed to be the reason for the observed results.

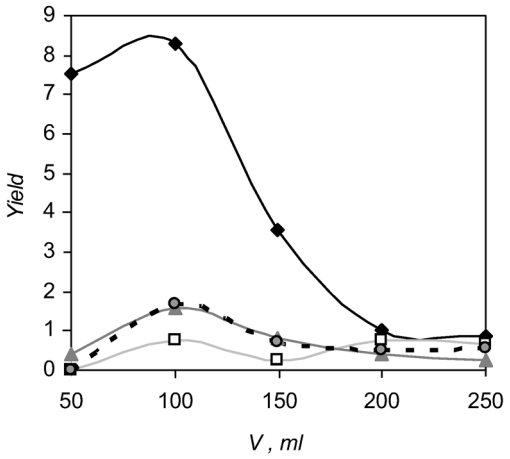

FIG. 5
Dependence of product yields (μmol g_{cat}^{-1}) on the volume (*V*) of the liquid phase: CH_4 (◆), CO (□), CH_3OH (▲), $H_2/100$ (●). The amount of formaldehyde formed in the liquid phase was under the detection limit. Conditions: irradiation time 24 h, 8 W Hg lamp, CO_2 pressure at carbonation 110 kPa, concentration of catalyst 1 g dm^{-3}

The catalyst in the annular space is not maintained in uplift, its particles gradually falling down to the bottom part of the reactor, which keeps the catalysts concentration not uniform and causes a scattering effect. This explanation was visually verified by an independent experiment in an identical glas reactor containing TiO_2 suspended in a methylorange solution for better visibility. Ballari et al.[14] concluded that perfect mixing is one of the most important pressumptions to avoid transport phenomena. This requirement is however often not fulfilled in laboratory reactors with a magnetic stirrer, even at high speeds of stirring. The volume of 100 ml corresponds to a situation when the end of the pen UV lamp is just at the upper reach of the solution. This means that the reactor configuration is not annular in this case. As soon as the volume of the liquid phase drops below 100 ml, a mean decrease in the yields is observed, caused probably by the too small volume of the liquid and/or a large distance of the liquid surface from the UV lamp.

CONCLUSIONS

In this paper, the effects of temperature, pressure and volume of the reacting phase on photocatalysis exemplified by CO_2 photoreduction at suspended nanocrystalline TiO_2 were studied. Similar to other photocatalytic reactions, the photocatalytic reduction of CO_2 is not also significantly sensitive to small variations in temperature (10 K). Experimental results demonstrate that the CO_2 pressure at the carbonation of the solution influenced the selectivity of CO_2 conversion to methane and methanol; the molecular hydrogen yield is hundred times higher and independent of the pressure. The observed dependence of the product yields on the volume of the liquid phase confirms the fact that perfect mixing is one of the most important factors required in photocatalytic slurry reactors, but difficult to obey for an annular configuration of the reactor.

The financial support of the Ministry of Education, Youth and Sports of the Czech Republic (research project NPV II 2B06068) is gratefully acknowledged. Ms. O. Šolcová and Ms. L. Matějová (Institute of Chemical Process Fundamentals, Academy of Science of the Czech Republic, Prague) are thanked for the preparation and characterisation of TiO_2.

REFERENCES

1. Hoffmann M. R., Martin S. T., Choi W., Bahnemann D. W.: *Chem. Rev.* **1995**, *95*, 69.
2. Fox M. A., Dulay M. T.: *Chem. Rev.* **1993**, *93*, 341.
3. Cant N. W., Cole J. R.: *J. Catal.* **1992**, *134*, 317.

4. Nakamura I., Negishi N., Kutsuna S., Ihara T., Sugihara S., Takeuchi K.: *J. Mol. Catal. A: Chem.* **2000**, *161*, 205.
5. Li F. B., Li X. Z., Ao C. H., Hou M. F., Lee S. C.: *Appl. Catal., B* **2004**, *54*, 275.
6. Heller A.: *Acc. Chem. Res.* **1995**, *28*, 503.
7. Cai R., Hashimoto K., Itoh K., Kubota Y., Fujishima A.: *Bull. Chem. Soc. Jpn.* **1991**, *64*, 1268.
8. Klusoň P., Lusková H., Červený L., Klisaková J., Cajthaml T.: *J. Mol. Catal. A: Chem.* **2005**, *242*, 62.
9. Ye W., Chen D., Gossage J., Li K.: *J. Photochem. Photobiol., A* **2006**, *183*, 35.
10. Du P., Moulijn J. A., Mul G.: *J. Catal.* **2006**, *238*, 342.
11. Hirano K., Inoue K., Yatsu T.: *J. Photochem. Photobiol., A* **1992**, *64*, 255.
12. Mizuno T., Adachi K., Ohta K., Saji A.: *J. Photochem. Photobiol., A* **1996**, *98*, 87.
13. Davies J. A., Boucher D. L., Edwards J. G.: *Adv. Photochem.* **1995**, *19*, 235.
14. Ballari M. M., Brandi R., Alfano O., Cassano A.: *Chem. Eng. J.* **2008**, *136*, 50.
15. Ballari M. M., Brandi R., Alfano O., Cassano A.: *Chem. Eng. J.* **2008**, *136*, 242.
16. Sasirekha N., Basha S. J. S., Shanthi K.: *Appl. Catal., B* **2006**, *62*, 169.
17. Tseng I.-H., Chang W.-C., Wu J. C. S.: *Appl. Catal., B* **2002**, *37*, 37.
18. Usabharatana P., McMartin D., Veawab A., Tontiwachwuthikul P.: *Ind. Eng. Chem. Res.* **2006**, *46*, 2558.
19. Anpo M., Yamashita H., Ichinashi Y., Ehara S.: *J. Electroanal. Chem.* **1995**, *396*, 21.
20. Kohno Y., Hayashi H., Takenaka S., Tanaka T., Funabiki T., Yoshida S.: *J. Photochem. Photobiol., A* **1999**, *126*, 117.
21. Kaneco S., Shimizu Y., Ohta K., Mizuno T.: *J. Photochem. Photobiol., A* **1998**, *115*, 223.
22. Adachi K., Ohta K., Mizuno M.: *Solar Energy* **1994**, *53*, 187.
23. Subrahmanyam M., Kaneco S., Alonso-Vante N.: *Appl. Catal., B* **1999**, *23*, 169.
24. Tan S. S., Zou L., Hu E.: *Catal. Today* **2006**, *115*, 269.
25. Tan S. S., Zou L., Hu E.: *Catal. Today* **2008**, *131*, 125.